A wavelength and lifetime responsive cryptate-containing fluorescent probe for zinc ions in water†

Cara E. Felton,[a] Lindsay P. Harding,[a] Jennifer E. Jones,[b] Benson M. Kariuki,[b] Simon J. A. Pope*[b] and Craig R. Rice*[a]

Received (in Cambridge, UK) 7th August 2008, Accepted 16th September 2008
First published as an Advance Article on the web 20th October 2008
DOI: 10.1039/b813775g

A diamino-functionalised cryptate can react irreversibly with butanal in water, in the presence of an excess of a metal ion, to form a cyclised bis-aminal complex, which displays metal-dependent luminescence properties.

It is now recognised that zinc is a metal of fundamental neurobiological and neuropathological importance.[1] Consequently, an understanding of its role in such contexts requires an ability to detect, track and image zinc ions. The physical and electronic nature of Zn^{2+} dictates that biological imaging of it is dominated by two main modes: optical fluorescence and magnetic resonance imaging. Confocal fluorescence microscopy can be exploited to image zinc at cellular levels,[2] and has driven the development and design of a range of molecular probes for the detection of zinc. The considerations for the photophysical attributes of such a probe are dictated by the optical properties of biological tissue: visible light sensitisation and emission are key for avoiding endogenous autofluorescence. Given the development of fluorescence lifetime imaging microscopy (FLIM),[3] it would also be desirable and pertinent to consider emission lifetime as an exploitable parameter since lifetime imaging is generally independent of probe concentration. Lifetime responsive probes for Ca^{2+} can be utilised in FLIM, but are disadvantaged since they require UV excitation.[4,5] To date, however, lifetime-responsive probes for zinc appear to be limited to lanthanide-based arrays where zinc binding modulates the resultant phosphorescence.[6]

The vast majority of luminescent probes for zinc have been based upon well studied organic dyes such as fluorescein,[7] quinoline[8] and coumarin[9] amongst other notable examples.[10] In this paper we report the development of a luminescent, responsive probe, based on a 2,2′-bipyridine functionalised cryptate core, which demonstrates variable wavelength (with large Stokes shift) and fluorescence lifetime responses upon complexation to a variety of metal ions, revealing an ability to detect zinc in ionically competitive aqueous solutions.

The cryptate **1** was synthesised in six steps from 6,6′-dimethyl-3,3′-diacetylamino-2,2′-bipyridine (see ESI for full synthetic scheme†) and was found to react with a variety of mono- and divalent metal cations, in either MeCN or H_2O to form the resultant complex $[\mathbf{1}\text{–}M]^{+/2+}$. As previously observed in similar systems, the amino groups react readily with aldehydes[11] and reaction of either the zinc or barium complex with an excess of butanal (non-volatile and water-soluble) results in cyclisation at the two amino groups forming the 7-membered bis-aminal species $[\mathbf{2}\text{–}M]^{+/2+}$ (Scheme 1)‡. Whilst this reaction can be carried out in both MeCN and H_2O, it is important to note that no reaction with butanal was observed with the metal-free ammonium cryptate species **1**, or in the presence of just one equivalent of metal ion. Previous studies have shown that the proximity of the amino groups to one another greatly affects their reactivity.[11] In the free cryptate, the bipyridine unit will be twisted away from planarity and we have shown that this type of geometrical arrangement results in unreactive amino groups. However, upon coordination with a metal ion, the bipyridine unit will be forced to approach planarity, facilitating the reaction will butanal and resulting in the formation of the bis-aminal species. Thus coordination of the cryptate unit is required for the reaction with butanal to occur. Excess metal ion is needed to act as a Lewis acid to promote the reaction.[11]

Both the cyclised zinc and barium complexes were characterised by ^1H NMR and HR ESI-MS and in the case of the latter complex, a single crystal X-ray structure was obtained (Fig. 1). In the crystal structure, the formation of the aminal species is confirmed with the barium ion coordinated by four

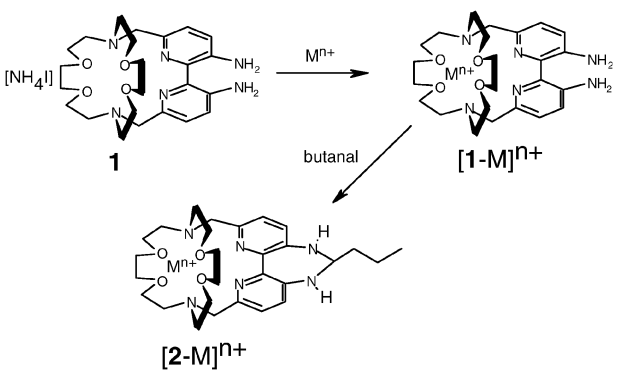

Scheme 1 Formation of $[\mathbf{1}\text{–}M]^{n+}$ and $[\mathbf{2}\text{–}M]^{n+}$.

[a] *Department of Chemical and Biological Sciences, University of Huddersfield, Huddersfield, UK HD1 3DH. E-mail: c.r.rice@hud.ac.uk; Fax: (+44) 148-447-2182; Tel: (+44)-148-447-3759*
[b] *School of Chemistry, Main Building, Cardiff University, Cardiff, UK CF10 3AT. E-mail: popesj@cardiff.ac.uk; Fax: (+44) 029-20874030; Tel: (+44) 029-20879316*

† Electronic supplementary information (ESI) available: Details of ligand synthesis, further photophysical measurements and data fitting details, crystallographic data and parameters associated with the structure of [**2**-Ba]$(ClO_4)_2$. CCDC 697886. For ESI and crystallographic data in CIF or other electronic format see DOI: 10.1039/b813775g

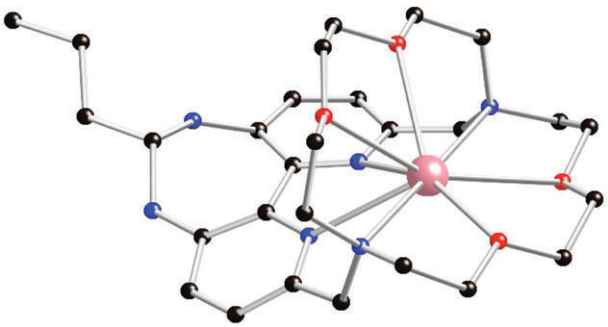

Fig. 1 X-Ray crystal structure of the cyclised barium complex cation, $[\mathbf{2}\text{–Ba}]^{2+}$. Coordinated counter ions and solvent molecules have been omitted for clarity.

oxygen atoms (2.809(5)–2.888(5) Å) and four nitrogen atoms (2.836(5)–2.911(5) Å) from the cryptate moiety, along with two oxygen atoms from the perchlorate counter ions (2.888(5) and 3.006(6) Å, omitted for clarity).

The unique reactivity of **1** imparts tunable optical and emissive properties. In its free diamino form, the probe (**1**) absorbs with λ_{max} = 317 nm (ε *ca.* 7500 M^{-1} cm^{-1}) and is weakly emissive at *ca.* 440 nm† in aerated aqueous solution. For comparison, a variety of metal cations (5×10^{-4} M as perchlorate salts) were added to a 1×10^{-4} M solution of **1** resulting in minor emission wavelength shifts together with general enhancements in emission intensity. Comparison of Fe^{3+} (physiologically, the trivalent state is the most prevalent) and Zn^{2+} was notable as these cations produced the most significant blue (λ_{em} = 428 nm) and red shifts (λ_{em} = 452 nm) respectively, thus allowing differentiation on the basis of wavelength. Further evidence of binding was observed in the absorption spectra where the lowest energy IL band is red shifted in comparison to **1**. In the case of $[\mathbf{1}\text{–Zn}]^{2+}$, absorption λ_{max} = 365 nm (ε *ca.* 8100 M^{-1} cm^{-1}). Further investigation showed that exposure of a 1×10^{-4} M solution of **1** to titrated micromolar concentrations of Zn^{2+} induced a >10-fold increase in emission intensity (see ESI†). The optical properties of the probe were further optimized by addition of excess butanal to the solutions of $[\mathbf{1}\text{–M}]^{n+}$, resulting in the formation of the cyclised bis-aminal complex species, $[\mathbf{2}\text{–M}]^{n+}$. This derivatisation rapidly resulted in the formation of a yellow coloured solution as a consequence of a red shift in the lowest energy absorption band. This was exemplified in the electronic spectrum of $[\mathbf{2}\text{–Zn}]^{2+}$ with λ_{max} = 439 (ε *ca.* 5700 M^{-1} cm^{-1}) and 282 (ε *ca.* 24 300 M^{-1} cm^{-1}) nm, demonstrating the dramatic low energy shift upon cyclisation, and thus facilitating visible sensitisation (λ_{ex} = 425 nm) of $[\mathbf{2}\text{–M}]^{n+}$ (see Fig. 2 for excitation and emission spectra of $[\mathbf{2}\text{–Zn}]^{2+}$). It is important to note that, in contrast, neither **1** nor $[\mathbf{1}\text{–M}]^{n+}$ are strongly absorbing above 420 nm and therefore excitation wavelengths at or above this represent genuine selectivity for the cyclised species. In its cyclised guise, the resultant photophysical responses of the various complexes were even more varied. Table 1 compiles the data associated with the wavelength and fluorescence lifetime responses (in the case of [**2**–M]) of the probes to the various metal ions, together with the relative intensity (compared to the zinc complex) of the resultant emission from $[\mathbf{2}\text{–M}]^{n+}$.

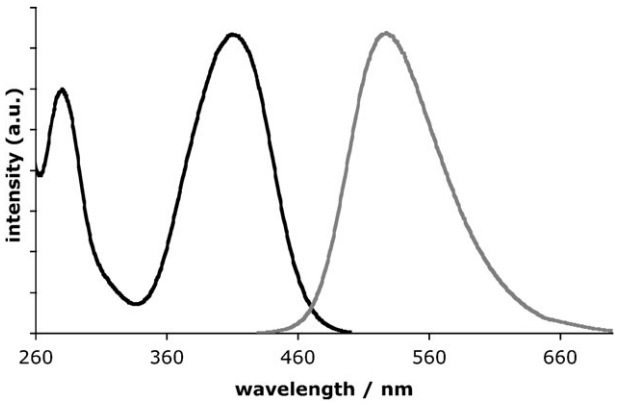

Fig. 2 Examples of excitation (left) and emission (right) spectra of $[\mathbf{2}\text{–Zn}]^{2+}$ obtained in aerated water.

Table 1 Luminescent properties of $[\mathbf{1}\text{–M}]^{n+}$ and $[\mathbf{2}\text{–M}]^{n+}$

M	[**1**–M]/nm[a]	[**2**–M]/nm[b]	Relative intensity (I/I_0)[c]	[**2**–M] τ/ns[d]
Li^+	442	559	0.03	1.3
Na^+	442	563	0.03	1.3
K^+	441	560	0.03	1.2
Mg^{2+}	440	560	0.03	1.3
Ca^{2+}	444	562	0.03	1.3
Ba^{2+}	437	543	0.23	9.0
Fe^{3+}	428	568	0.16	1.0
Co^{2+}	440	556	0.07	1.5
Ni^{2+}	440	566	0.05	1.4
Cu^{2+}	Weak	Weak	—	—
Zn^{2+}	452	533	1	5.9
Cd^{2+}	442	528	0.29	5.3
Hg^{2+}	441	520 weak	0.01	—

[a] λ_{ex} = 350 nm. [b] λ_{ex} = 425 nm. [c] Where I = M + **2**, I_o = Zn + **2**. [d] λ_{ex} = 372 or 459 nm. Measurements obtained using 1×10^{-4} M of **1** and 5×10^{-4} M M^{n+}. All solutions were allowed to equilibrate for 10 min and the pH remained between 6.5 and 7.5 in all cases. For $[\mathbf{2}\text{–M}]^{+/2+}$, samples were re-recorded after 24 h, demonstrating no further changes.

The response to zinc produced the most intense emission by a significant margin†. Generally, the emission maxima from the cyclised diimine lumophore lie between 515 and 570 nm following excitation in the visible at 425 nm (although as demonstrated in Fig. 2, excitation was possible above 450 nm; see also fluorescence lifetime measurements utilizing 459 nm excitation), indicating a significant and desirable Stokes shift more commonly associated with emissive transition metal complexes. The dramatic increase in luminescence intensity upon coordination to zinc ions, when compared to the other metal cations, can be attributed to a number of factors. Zn^{2+} not only has a higher affinity for the bipyridine unit than the Group 1 and 2 cations, it also has a closed shell d^{10} configuration whereas the paramagnetic metal ions (Ni^{2+}, Co^{2+}, Cu^{2+}) are typically efficient quenchers. Comparison with the other conjoiners of the Group 10 metal ions reveals a gradual decrease in luminescence intensity down the group, which can be attributed to quenching *via* the heavy atom effect.[12]

The fluorescence lifetime of $[\mathbf{2}\text{–Zn}]^{2+}$ (5.9 ns, Fig. 3) is far longer than those species that emit at *ca.* 560 nm (Ca^{2+}, Ni^{2+}, Mg^{2+}, K^+, Na^+, Li^+, Co^{2+} and Fe^{3+}). For analytes of

This journal is © The Royal Society of Chemistry 2008

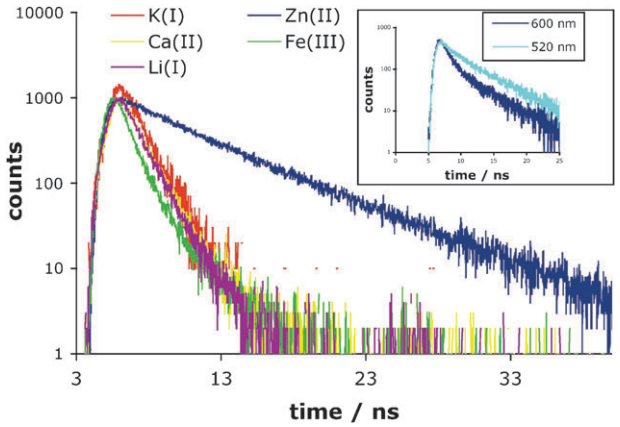

Fig. 3 Comparative luminescence lifetime decay profiles of $[\mathbf{2}–M]^{n+}$ where M = K(I), Zn(II), Fe(III), Ca(II), Li(I). Inset: wavelength dependent lifetime decays of $[\mathbf{2}–M]^{n+}$ in an ionic mixture. Data fits and residuals are omitted for clarity.

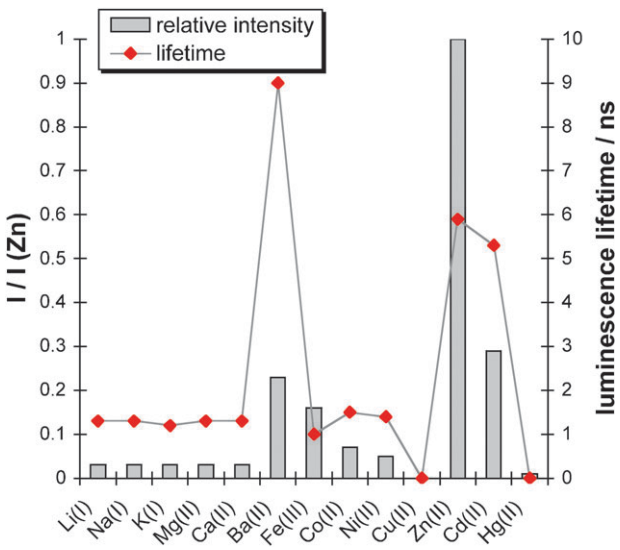

Fig. 4 Graphical summary of the luminescence responses of the cyclised cryptate species $[\mathbf{2}–M]^{n+}$ in water.

biological relevance, this lifetime dependence allows screening for zinc in an ionically competitive (4 mM $ZnCl_2$ in 140 mM NaCl, 4mM KCl, 1.2 mM $MgCl_2$, 2.3 mM $CaCl_2$) buffered (HEPES) aqueous medium at pH 7.4.[13] Fig. 3 inset shows two lifetime traces obtained as a function of wavelength detection (520 and 600 nm) following formation of $[\mathbf{2}–M]^{+/2+}$ in the ionic mixture. With reference to Table 1, one would assume that the decay profiles are multi-component, but due to the similarity of the shorter lifetime components, the profiles were satisfactorily fitted with bi-exponentials in all cases. At longer wavelengths (>550 nm), the shorter lifetime contributions (*ca.* 1.3 ns) of Na^+, K^+, Mg^{2+} and Ca^{2+} are noted, but superimposed on a long-lived component. In contrast, at lower wavelengths (<550 nm), the contribution of the long-lived emission (*ca.* 5.9 ns) is dominant, correlating with the presence of the highly emissive zinc complex (see Table 1 and ESI†). Thus, for species $[\mathbf{2}–M]^{n+}$, luminescence lifetime measurements can be used as a discriminatory technique (Fig. 4) for detection of zinc even in an ionic background that may prevent conventional steady state wavelength analysis.

We acknowledge support from the Universities of Cardiff and Huddersfield and EPSRC (EP/E048390/1).

Notes and references

‡ Synthesis of $[\mathbf{2}–Zn](ClO_4)_2$: in a typical experiment, to the ammonium cryptate $[\mathbf{1}NH_4]I$ (5 mg, 8.1×10^{-3} mmol) in MeCN (1 ml) was added an excess of $Zn(ClO_4)_2{\cdot}6H_2O$ (15 mg, 4.0×10^{-2} mmol) and one drop of butanal. Diethyl ether was then slowly diffused in over 24 h. After this time, orange crystals were deposited, which were collected by filtration (3 mg, 47%). ^{1}H NMR (500 MHz, CD_3CN) δ_H 7.48 (d, $^3J_{HH}$ = 8.4 Hz, 2H), 7.22 (d, $^3J_{HH}$ = 8.4 Hz, 2H), 5.91 (s, 2H, NH), 4.15 (m, 1H, $CH_3CH_2CH_2CH$–), 4.01 (m, 4H), 3.74–3.32 (m, overlapping, 18H), 3.15 (m, 2H), 2.87 (m, 4H), 1.86 (m, 2H, $CH_3CH_2CH_2CH$–), 1.56 (m, 2H, $CH_3CH_2CH_2CH$–), 0.97 (t, $^3J_{HH}$ = 7.3 Hz, 3H, $CH_3CH_2CH_2CH$–). ESI-MS found *m*/*z* 689 $\{[\mathbf{2}Zn]ClO_4\}^+$; HR ESI-MS found 689.2018, $C_{28}H_{42}ClN_6O_8Zn$ requires 689.2038 (error 2.89 ppm). $[\mathbf{2}–Ba](ClO_4)_2$: ^{1}H NMR (500 MHz, CD_3CN) δ_H 7.30 (d, $^3J_{HH}$ = 8.2 Hz, 2H, py), 7.14 (d, $^3J_{HH}$ = 8.2 Hz, 2H, py), 5.50 (d, $^3J_{HH}$ = 3.6 Hz, 2H, –NH), 4.33 (m, 1H, $CH_3CH_2CH_2CH$–), 4.16 (d, $^3J_{HH}$ = 13.6 Hz, 2H), 3.78–3.57 (m, overlapping, 14H), 3.28 (m, 2H), 3.10 (m, 2H), 2.94 (m, 2H), 2.78 (m, 2H), 2.65 (m, 2H), 2.53 (m, 2H), 1.77 (m, 2H, $CH_3CH_2CH_2CH$–), 1.52 (m, 2H, $CH_3CH_2CH_2CH$–), 0.95 (t, $^3J_{HH}$ = 7.3 Hz, 3H, $CH_3CH_2CH_2CH$–). ESI-MS found *m*/*z* 736 $\{[\mathbf{2}Ba]ClO_4\}^+$; HR ESI-MS found 736.1781, $C_{28}H_{42}BaClN_6O_8$ requires 763.1799 (error 2.4 ppm).

1 (*a*) E. L. Que, D. W. Domaille and C. J. Chang, *Chem. Rev.*, 2008, **108**, 1517; (*b*) K. Kikuchi, K. Komatsu and T. Nagano, *Curr. Opin. Chem. Biol.*, 2004, **8**, 182; (*c*) C. J. Chang and S. J. Lippard, *Met. Ions Life Sci.*, 2006, **1**, 321.

2 C. J. Chang, J. Jaworski, E. M. Nolan, M. Sheng and S. J. Lippard, *Proc. Natl. Acad. Sci. U. S. A.*, 2004, **101**, 1129.

3 For a general overview of FLIM see J. R. Lakowicz, in *Principles of Fluorescence Spectroscopy*, 3rd edn, 2006, and references therein.

4 N. Miyoshi, K. Hara, S. Kimura, K. Nakanishi and M. Fukuda, *Photochem. Photobiol.*, 1991, **53**, 415.

5 For example see J. R. Lakowicz, H. Szmacinski, K. Nowaczyk and M. L. Johnson, *Cell. Calcium*, 1992, **13**, 131.

6 S. J. A. Pope and R. H. Laye, *Dalton Trans.*, 2006, 3108.

7 For examples see (*a*) G. K. Walkup, S. C. Burdette, S. J. Lippard and R. Y. Tsien, *J. Am. Chem. Soc.*, 2000, **122**, 5644; (*b*) S. C. Burdette, G. K. Walkup, B. Springler, R. Y. Tsien and S. J. Lippard, *J. Am. Chem. Soc.*, 2001, **123**, 7831; (*c*) S. C. Burdette, C. J. Frederickson, W. Bu and S. J. Lippard, *J. Am. Chem. Soc.*, 2003, **125**, 1778; (*d*) C. R. Goldsmith and S. J. Lippard, *Inorg. Chem.*, 2006, **45**, 555; (*e*) K. Komatsu, K. Kikuchi, H. Kojima, Y. Urano and T. Nagano, *J. Am. Chem. Soc.*, 2005, **127**, 10197.

8 For a recent overview see: (*a*) Z. Dai and J. W. Canary, *New J. Chem.*, 2007, **31**, 1708; (*b*) L. Xue, H.-H. Wang, X.-J. Wang and H. Jiang, *Inorg. Chem.*, 2008, **47**, 4310; (*c*) H.-H. Wang, Q. Gan, X.-J. Wang, L. Xue, S.-H. Liu and H. Jiang, *Org. Lett.*, 2007, **9**, 4995.

9 For example (*a*) K. Komatsu, Y. Urano, H. Kojima and T. Nagano, *J. Am. Chem. Soc.*, 2007, **129**, 13447; (*b*) N. C. Lim, J. V. Schuster, M. C. Porto, M. A. Tanudra, L. Yao, H. C. Freake and C. Bruckner, *Inorg. Chem.*, 2005, **44**, 2018.

10 (*a*) M. M. Henary, Y. Wu and C. J. Fahrni, *Chem.–Eur. J.*, 2004, **10**, 3015; (*b*) M. D. Shults, D. A. Pearce and B. Imperiali, *J. Am. Chem. Soc.*, 2003, **125**, 10591; (*c*) E. Van Dongen, L. M. Dekkers, K. Spijker, E. W. Meijer, L. Klomp and M. Merkx, *J. Am. Chem. Soc.*, 2006, **128**, 10754.

11 H. J. Clayton, L. P. Harding, J. P. Irvine, J. C. Jeffery, T. Riis-Johannessen, A. P. Laws, C. R. Rice and M. Whitehead, *Chem. Commun.*, 2008, 108.

12 A. E. Dennis and R. C. Smith, *Chem. Commun.*, 2007, 4641.

13 O. Reany, T. Gunnlaugsson and D. Parker, *Chem. Commun.*, 2000, 473.